

# Formate to Oxalate: A Crucial Step for the Conversion of Carbon Dioxide into Multi-carbon Compounds

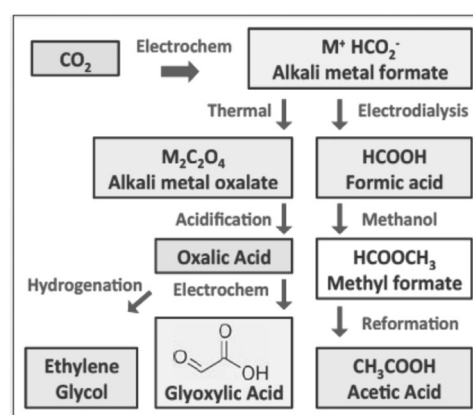
Prasad S. Lakkaraju,<sup>\*,[b]</sup> Mikhail Askerka,<sup>[a]</sup> Heidie Beyer,<sup>[b]</sup> Charles T. Ryan,<sup>[b]</sup> Tabbetha Dobbins,<sup>[c]</sup> Christopher Bennett,<sup>[c]</sup> Jerry J. Kaczur,<sup>[d]</sup> and Victor S. Batista<sup>\*,[a]</sup>

The efficient conversion of formate into oxalate could enable the industrial-scale synthesis of multi-carbon compounds from CO<sub>2</sub> by C–C bond formation. We found conditions for the highly selective catalytic conversion of molten alkali formates into pure solid oxalate salts. Nearly quantitative conversion was accomplished by calcination of sodium formates with sodium hydride. A catalytic mechanism proceeding through a carbonite intermediate, generated upon H<sub>2</sub> evolution, was supported by density functional theory calculations, Raman spectroscopy, and the observed changes in the catalytic performance upon changing the nature of the base or the reaction conditions. Whereas the conversion of formate into oxalate by using a hydroxide ion catalyst was previously studied, hydride ion catalysis and the chain reaction mechanism for the conversion involving a carbonite ion intermediate are reported herein for the first time.

The production of chemicals and fuels from CO<sub>2</sub> could provide a viable solution to challenges of global relevance. Reducing the amount of CO<sub>2</sub> in the atmosphere could mitigate global warming. Converting CO<sub>2</sub> into fuels could produce carbon-neutral renewable fuels for energy storage, whereas synthesizing multi-carbon chemicals from CO<sub>2</sub> could enable the sustainable production of precursors or feedstocks for organic synthesis.<sup>[1,2]</sup> Therefore, there is great interest in the conversion of CO<sub>2</sub> into formate and oxalate products.<sup>[3–10]</sup> However, economically viable and environmentally benign methods are yet to be established. Outstanding challenges include Faradaic efficiency,

electrocatalyst stability, product selectivity, isolation, and purification of the products.

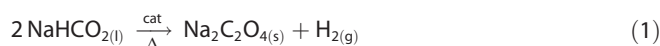
Over the past six years, research at Liquid Light, Inc., has been focused on the development of electrochemical and chemical methods for the conversion of CO<sub>2</sub> into value-added products on a large scale.<sup>[11–14]</sup> Scheme 1 illustrates some of the pathways of interest for the bulk synthesis of C<sub>2</sub> compounds from CO<sub>2</sub>, relying upon the conversion of formate into oxalate,



Scheme 1. Conversion of CO<sub>2</sub> into value-added products.

including synthetic routes for the production of highly utilized chemicals such as ethylene glycol and glyoxylic acid. The pathways are particularly attractive, as an efficient method for the generation of alkali metal formates by electrochemical reduction of CO<sub>2</sub> was previously demonstrated.<sup>[11]</sup> Specifically, potassium and sodium formates were produced with Faradaic efficiencies > 60% in 100 cm<sup>2</sup> cells, with current densities as high as 120 mA cm<sup>-2</sup> and cell potentials lower than 4 V.<sup>[11,12]</sup> Alkali metal formate salts may be converted into formic acid by either electrolysis or electrochemical acidification (Scheme 1).

Whereas formic acid has been explored as a fuel and in applications to commercial chemistry, the development of viable synthetic routes to generate C<sub>2</sub> and higher-order carbon compounds from formate salts remains an outstanding challenge. In this communication, we report a highly useful catalytic conversion of formates into oxalates [Eq. (1)]:



[a] M. Askerka, Prof. V. S. Batista  
Department of Chemistry  
Yale University  
225 Prospect St., New Haven, CT 06520-8107 (USA)  
E-mail: victor.batista@yale.edu

[b] Prof. P. S. Lakkaraju, H. Beyer, C. T. Ryan  
Chemistry & Biochemistry Department  
Georgian Court University  
900 Lakewood Ave., Lakewood, NJ 08701 (USA)  
E-mail: Lakkaraju@georgian.edu

[c] Dr. T. Dobbins, C. Bennett  
Department of Physics  
Rowan University  
201 Mullica Hill Road, Glassboro, NJ 08028 (USA)

[d] J. J. Kaczur  
Liquid Light, Inc.  
11 Deer Park Drive, Suite 121, Monmouth Junction, NJ, 08852 (USA)

Supporting Information for this article can be found under <http://dx.doi.org/10.1002/cctc.201600765>.

with high selectivity for C–C coupling chemistry achieved by calcination with alkali hydroxide or hydride catalysts. The two main products,  $\text{H}_{2(g)}$  and  $\text{Na}_2\text{C}_2\text{O}_{4(s)}$ , are spontaneously separated, which makes the synthetic process simple and practical if byproducts such as carbon monoxide and carbonates are curtailed, as in a recently disclosed integrated process.<sup>[13, 14]</sup>

The conversion of formate into oxalate has been a long-standing challenge.<sup>[15–21]</sup> Thermal approaches were explored<sup>[16]</sup> and factors determining the conversion efficiency into oxalates and other byproducts were analyzed by using varying amounts of sodium hydroxide under various temperatures and partial vacuum conditions.<sup>[17]</sup> Products of decomposition including carbonates, oxalates, CO, and  $\text{CO}_2$  were determined from dynamic thermoanalytical analysis of the thermal decomposition of  $\text{LiHCO}_2$ ,  $\text{NaHCO}_2$ ,  $\text{KHCO}_2$ ,  $\text{RbHCO}_2$ , and  $\text{CsHCO}_2$ .<sup>[18]</sup> However, conditions for achieving high product yields have yet to be established. For example, Baraldi<sup>[19]</sup> analyzed the IR spectra of 12 metal formates under heating in air at atmospheric pressure and under a dynamic vacuum of 1.3 Pa. Formation of oxalate was suggested by IR spectroscopy features upon heating formate under vacuum at 300 °C. However, decomposition into carbonate was observed at 475 °C.

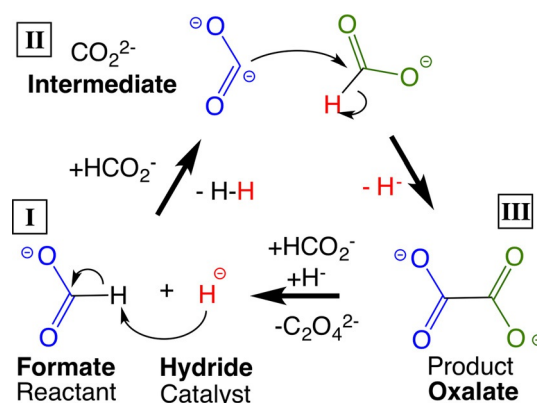
Górski<sup>[20, 21]</sup> explored the influence of gaseous and solid reactants on the yields of oxalates and carbonates during thermal decomposition of  $\text{LiHCO}_2$ ,  $\text{NaHCO}_2$ , and  $\text{KHCO}_2$ . Addition of  $\text{NaBH}_4$  to  $\text{NaHCO}_2$  resulted in 88% conversion yield, which declined to 0% conversion upon using a 1:1 molar ratio. Thus, reaction conditions for quantitative yields have not been reported. In addition, the underlying reaction mechanism remains uncertain. Whereas Górski proposed oxalate formation upon decomposition of formate as follows [Eq. (2) and (3)]:



it remains to be explored whether such a reaction, or an alternative mechanism, is consistent with theoretical studies and direct comparisons with experimental measurements, as reported below.

### Reaction times and product yields

We found reaction conditions for the best yield conversion of formate into oxalate upon melting alkali formate salts at high temperatures in the presence of a strong base, such as NaH or NaOH, by varying both the catalyst amount and the temperature. A porous solid, self-rising  $\text{NaC}_2\text{O}_4$  was produced as hydrogen gas evolved as a byproduct. DFT calculations supported a mechanism based on a hydride catalytic pathway (Scheme 2), consistent with Raman spectroscopy and the observed changes in the reaction times and product yields produced by changing the base (e.g., NaH or NaOH) or the reaction conditions. In particular, the reaction times were much shorter for the stronger base (NaH) than for NaOH at the same temperature. These observations are consistent with a rate-limiting step owing to the primary deprotonation of formate



**Scheme 2.** Catalytic conversion of formate into oxalate. Using the hydride base, 1 mol of formate is converted into a carbonite ion (blue color) that nucleophilically attacks the second mole of formate to release the hydride catalyst.

upon  $\text{H}_2$  evolution, followed by C–C bond formation (see below).

Table 1 (NaOH) reports the product yields obtained for different reaction times with NaH and NaOH. We found nearly quantitative conversion into oxalate for NaH and yields > 80% with NaOH at 390 °C but negligible conversion at lower temperatures (below 350 °C).

**Table 1.** Formate to oxalate conversion yields obtained by using NaH and NaOH as catalysts for various experimental conditions of temperature and reaction times under a  $\text{N}_2$  atmosphere.

Catalyst	Sample number	$T$ [°C]	Calcination time [min]	Catalyst [wt %]	Oxalate yield ( $\pm 1\%$ ) [%]
NaH	1	390	10	2	92
	2	390	10	2	99
	3	390	8	2	93
NaOH	1	390	20	2.5	74
	2	390	30	2.5	68
	3	390	40	2.5	86
	5	350	15	0	0.9
	6	350	30	0	0.5

Shorter reaction times, higher product yields, and superior quality of the oxalate product were obtained upon using NaH as a catalyst (Table 1, NaH). In contrast, NaOH-catalyzed reactions typically yielded a mixture of products, including oxalate, carbonate, carbon monoxide, and hydrogen. The maximum oxalate yield, obtained with NaOH, was approximately 80%, including as much as 10% carbonate. The reaction times were typically four times longer for NaOH than for NaH. If the formate to oxalate conversion was performed by using NaH or NaOH at temperatures > 420 °C, charring of the sample occurred, which affected the quality of the product.

In addition, we found that the nature of the alkali metal ion significantly affected the product yield and the optimum reaction conditions. For comparison, Table 2 reports the product yields obtained with (or without) KOH by calcination at 420–480 °C for various reaction times. Clearly, KOH increased the

**Table 2.** Formate to oxalate conversion yields obtained by using KOH as a catalyst for various reaction times at 420–520 °C under a N<sub>2</sub> atmosphere.

Sample number	T [°C]	Calcination time [min]	KOH added [wt%]	Oxalate yield (±1%) [%]
1	420	30	0	8
2	420	30	5	76
3	420	30	8	74
4	420	45	8	74
5	420	60	5	78
6	440	30	0	14
7	440	30	8	77
8	440	60	5	78
9	480	30	0	73
10	480	30	2	76
11	520	5	0	71

yield obtained at 420–440 °C, although it required higher temperature than either NaOH or NaH to obtain yields > 75%. At higher temperatures (> 500 °C), the reaction yields were not affected by the addition of a catalyst and the reaction times were significantly reduced, even without addition of a catalyst base.

### Formate to oxalate conversion mechanism

DFT calculations supported a simple mechanism (Scheme 2), initiated by hydrogen evolution and the formation of the carbonite (CO<sub>2</sub><sup>2-</sup>) intermediate, upon reaction of formate with the hydride catalyst. Carbonite reacted with formate to produce oxalate by C–C bond formation, which regenerated the hydride catalyst.

We probed the catalytic thermal conversion of formate into oxalate by Raman spectroscopy at 350 °C (i.e., the highest temperature allowed by our variable-temperature system). As the reaction proceeded, we monitored the bands at  $\tilde{\nu}$  = 1357, 1072, and 770 cm<sup>-1</sup> (see the Supporting Information) assigned to the CO<sub>2</sub> symmetric stretch, formate C–H bending, and CO<sub>2</sub> bending, respectively. Simultaneously, two bands emerged at  $\tilde{\nu}$  = 1457 and 884 cm<sup>-1</sup> assigned to the oxalate C–O symmetric stretch and oxalate C–C stretch, respectively. The bands observed for the products were identical to those observed for an authentic sample of sodium oxalate.

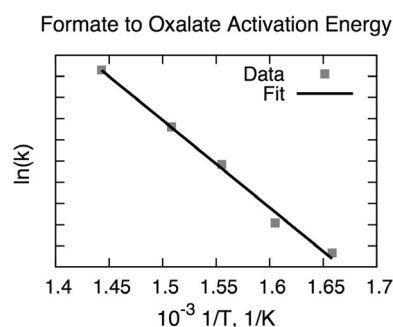
The experimental Raman band at  $\tilde{\nu}$  = 1076 cm<sup>-1</sup> was assigned to the O–C–O symmetric stretch of the carbonite intermediate, supported by DFT calculations (Supporting Information) and with the steady-state concentration of carbonite established during the course of the catalytic reaction upon continuous purging of H<sub>2(g)</sub> with N<sub>2(g)</sub> in the variable-temperature system. Another observation that supported the assignment to carbonite was that the intensity of the  $\tilde{\nu}$  = 1076 cm<sup>-1</sup> band diminished upon exposure of the sample to air or water, which enhanced the intensity of the oxalate bands. The intensity of the  $\tilde{\nu}$  = 1076 cm<sup>-1</sup> band was also correlated to hydrogen evolution during the course of the reaction and increased upon increasing the concentration of the hydride catalyst, as expected for an increased steady-state concentration of carbonite.

The formation of oxalate from the reaction of carbonite with water (Table 3, reaction k) was likely spontaneous, because of a large negative Gibbs free energy predicted for the reaction by DFT. We are currently conducting additional Raman spectroscopy studies on the reaction by using <sup>2</sup>H and <sup>13</sup>C isotope enriched formate samples, and the results of these investigations will be reported in a future publication.

**Table 3.** Reaction free energies in aqueous solution for various possible elementary steps associated with the conversion of formate into oxalate.

Reaction	$\Delta G_r$ [kcal mol <sup>-1</sup> ]			
	No ion	Na <sup>+</sup>	K <sup>+</sup>	
a	2 HCO <sub>2</sub> <sup>-</sup> → C <sub>2</sub> O <sub>4</sub> <sup>2-</sup> + H <sub>2</sub>	8	-1	2
a <sup>TS</sup>	2 HCO <sub>2</sub> <sup>-</sup> → [TS <sub>1</sub> ] <sup>‡</sup> → C <sub>2</sub> O <sub>4</sub> <sup>2-</sup> + H <sub>2</sub>	-	70	72
b	HCO <sub>2</sub> <sup>-</sup> → HO <sup>-</sup> + CO	21	21	25
c	HCO <sub>2</sub> <sup>-</sup> → H <sup>-</sup> + CO <sub>2</sub>	35	33	35
d	HO <sup>-</sup> + HCO <sub>2</sub> <sup>-</sup> → H <sub>2</sub> O + CO <sub>2</sub> <sup>2-</sup>	52	33	30
e	H <sup>-</sup> + HCO <sub>2</sub> <sup>-</sup> → H <sub>2</sub> + CO <sub>2</sub> <sup>2-</sup>	32	15	14
e <sup>TS</sup>	H <sup>-</sup> + HCO <sub>2</sub> <sup>-</sup> → [TS <sub>2</sub> ] <sup>‡</sup> → H <sub>2</sub> + CO <sub>2</sub> <sup>2-</sup>	35 <sup>[a]</sup>	28	26
f	HCO <sub>2</sub> <sup>-</sup> + CO <sub>2</sub> <sup>2-</sup> → H <sup>-</sup> + C <sub>2</sub> O <sub>4</sub> <sup>2-</sup>	-26	-18	-14
g	HO <sup>-</sup> + 2 HCO <sub>2</sub> <sup>-</sup> → H <sub>2</sub> O + H <sup>-</sup> + C <sub>2</sub> O <sub>4</sub> <sup>2-</sup>	26	16	16
h	H <sub>2</sub> O + H <sup>-</sup> → H <sub>2</sub> + OH <sup>-</sup>	-18	-16	-14
i	2 HCO <sub>2</sub> <sup>-</sup> → CO <sub>2</sub> + CO <sub>2</sub> <sup>2-</sup> + H <sub>2</sub>	69	50	53
j	CO <sub>2</sub> + CO <sub>2</sub> <sup>2-</sup> → C <sub>2</sub> O <sub>4</sub> <sup>2-</sup>	-61	-51	-49
k	2 CO <sub>2</sub> <sup>2-</sup> + 2 H <sub>2</sub> O → C <sub>2</sub> O <sub>4</sub> <sup>2-</sup> + 2 HO <sup>-</sup> + H <sub>2</sub>	-95	-67	-58

[a] Steps (e) and (f) are found to be crucial in the oxalate formation. Detailed mechanism is presented in Figure 2.

**Figure 1.** Eyring–Polanyi graph for the thermal conversion of sodium formate into sodium oxalate in the 330–420 °C temperature range by using sodium hydride as a catalyst base (2.5% by mass).

The temperature dependence of the reaction rates, shown in Figure 1, allowed for estimation of the activation enthalpy and activation entropy, according to the Eyring–Polanyi equation. The slope of the plot (Figure 1) yielded an activation enthalpy of 41 kcal mol<sup>-1</sup>, and the intercept corresponded to an activation entropy of -6 cal K<sup>-1</sup> mol<sup>-1</sup>. As discussed below, these results are fully consistent with the mechanism introduced in Scheme 2, as supported by DFT calculations of the reaction free-energy profile and direct comparison to experimental data.

DFT exploration of low free-energy pathways supported the proposed reaction mechanism, shown in Scheme 2, as indicated by the thermodynamics of the elementary steps summar-

ized in Table 3 (details of the DFT methodology are given in the Supporting Information).

We first analyzed the thermodynamics of the formate to oxalate conversion in terms of the simplest possible mechanism, that is, the direct reaction of two formate ions in the absence of the catalyst base (Table 3, reaction a). We found that although the reaction was certainly thermodynamically feasible, it was kinetically hindered (with a high-energy barrier  $> 70$  kcal mol<sup>-1</sup>) if it led to H<sub>2</sub> evolution through a single transition state. Oxalate formation according to Equations (2) and (3), as suggested by Gorski<sup>[20,21]</sup> (Table 3, reactions i and j), was also found to be thermodynamically unfavorable owing to the decomposition of formate into carbonite and carbon dioxide (Table 3, reaction i). Therefore, alternative reaction pathways were explored, including the pathway outlined in Scheme 2 for which the catalyst plays an important role.

The proposed mechanism is consistent with the various outcomes under the different experimental conditions. We note that a small amount of oxalate was obtained at 420 °C (8% yield) even without the addition of any kind of catalyst base, and higher yields ( $> 70\%$ ) were produced without a catalyst at higher temperatures ( $> 480$  °C) (Table 2). However, at lower temperatures (e.g., 420 °C), obtaining significant yields required the addition of a base. Also, the resulting product yields were quite different upon using NaH, NaOH, or KOH (Tables 1 and 2). These observations are all consistent with generation of the base catalyst in situ at higher temperatures ( $> 480$  °C). In particular, the catalyst base HO<sup>-</sup> can be generated by thermal decomposition of formate (Table 3, reaction b). The reaction involves free energy changes of 21 and 25 kcal mol<sup>-1</sup> for the sodium and potassium salts, respectively.

Formation of hydride by thermal decomposition of formate could be ruled out, as it was found to be thermodynamically a lot more demanding (Table 3, reaction c). However, hydride catalytic species could be readily generated from HO<sup>-</sup> upon reaction with formate (Table 3, reaction g). These results are thus consistent with generation of the hydride catalyst base in situ from HO<sup>-</sup> at high temperatures. Formate to oxalate conversion proceeds according to Scheme 2 (Table 3, reactions e and f) after generation of the H<sup>-</sup> catalyst. A detailed mechanism is described by the DFT free-energy profile shown in Figure 2.

Figure 2 (top panel) shows that the first step (I<sub>1</sub>→I<sub>2</sub>) involves electrostatic complexation of NaH (or KH) with formate. Then, H<sub>2</sub> evolves upon nucleophilic attack of hydride on formate (I<sub>2</sub>→I<sub>3</sub>). The transition state TS<sub>1</sub> is reached through rotation of the sodium (or potassium) hydride fragment, which relaxes into the weakly bound H<sub>2</sub>+CO<sub>2</sub>Na<sub>2</sub> intermediate, I<sub>3</sub>. The H<sub>2</sub> fragment spontaneously exchanges with formate (I<sub>4</sub>) to form the more stable intermediate I<sub>5</sub>.

Our calculations of the complete thermodynamic cycle (Supporting Information, Tables S1 and S2) show that I<sub>2</sub>→TS<sub>1</sub> is the rate-limiting step for oxalate formation (Table S2) with a barrier of 41.0 kcal mol<sup>-1</sup>, which is in excellent agreement with the experimental value estimated from the observed temperature dependence (Figure 1).

Figure 2 (top panel) shows that out-of-plane rotation of formate in I<sub>5</sub> brings together the two carbon atoms; this results

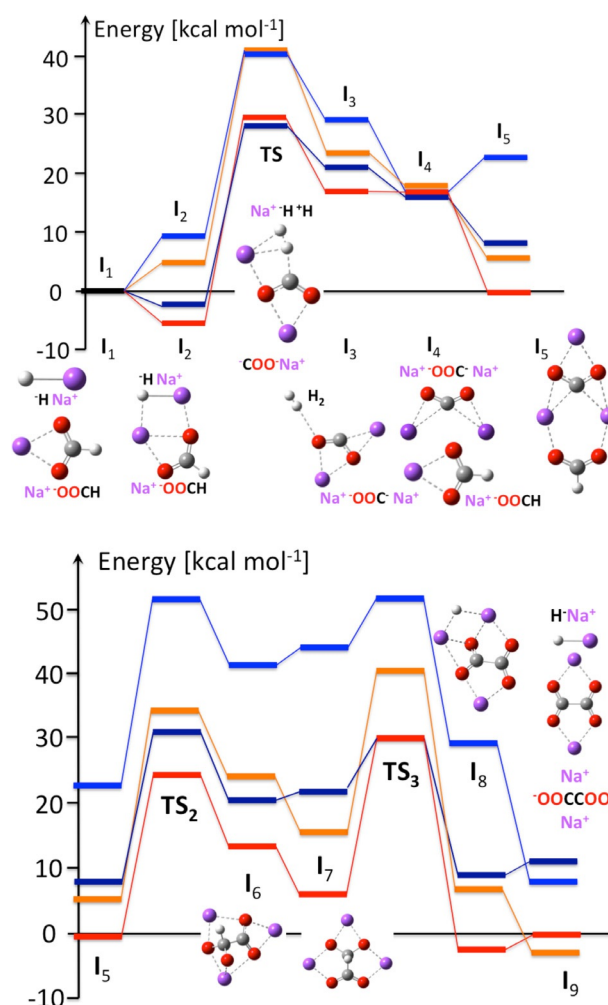


**Figure 2.** Free-energy profile of the catalytic conversion of formate into oxalate as salts of sodium (red 663 K, orange 298 K) and potassium (navy 713 K, blue 298 K) computed at the DFT B3LYP level of theory (see the Supporting Information).

in the formation of the transition state TS<sub>2</sub>, which forms the C–C bond in the (OOCHCOO)Na<sub>3</sub> complex (I<sub>6</sub>) before relaxing into the isomeric complex I<sub>7</sub> through 90° rotation of the O–C–C–O torsion angle and a slight rearrangement of the Na<sup>+</sup> counterions. The C–H bond is then elongated, which results in the formation of NaH+Na<sub>2</sub>C<sub>2</sub>O<sub>4</sub> (I<sub>8</sub>) through the transition state TS<sub>3</sub>. The separation of these electrostatically bound species, upon precipitation of Na<sub>2</sub>C<sub>2</sub>O<sub>4(s)</sub>, forms I<sub>9</sub> and regenerates NaH for the next turn of the catalytic cycle.

We found that quantitative conversion of formate into oxalate could be achieved by simple calcination of molten formate salts in the presence of NaH. DFT calculations supported a simple mechanism through a carbonite intermediate, generated upon H<sub>2</sub> evolution by reaction of formate with the catalytic hydride. The mechanism was found to be consistent with the thermodynamic parameters, which were obtained from temperature-dependence analysis and Raman spectroscopy of the carbonite intermediate. The reported findings are particularly relevant for industrial-scale generation of multi-carbon

compounds from CO<sub>2</sub>, as formate can be efficiently generated by electrochemical reduction of CO<sub>2</sub>.

Further, we are currently investigating the stability and reactivity of carbonite ions by analysis of <sup>13</sup>C- and <sup>2</sup>H-enriched samples by Raman spectroscopy and DFT studies. These studies could have a significant impact on the utilization of formate as a potential carboxylating reagent via carbonite nucleophiles.

## Experimental Section

The thermal reactions were explored by using a Thermo Scientific Thermolyne Benchtop Muffle Furnace that could reach a maximum temperature of 1200 °C. Reactions were performed under a flowing N<sub>2</sub> atmosphere by introducing N<sub>2</sub> gas through a vent port, as oxygen lowered the yield of oxalate formed. A series of experiments were designed by using reaction temperature, reaction time, and the amount of catalyst as the reaction condition variables to obtain the best possible yields. A typical bench-scale reaction was conducted by using a formate sample (4.0 g) placed into a 50 mL nickel crucible, which was then calcined between 300–480 °C. All chemicals were reagent grade and were obtained from Sigma-Aldrich, including NaOH, sodium hydride, KOH, sodium and potassium formate, sodium and potassium oxalate, sulfuric acid, and potassium permanganate (J. T. Baker). The catalyst (e.g., NaH, NaOH, KOH) in weighed amounts of 2.5% by mass were mixed thoroughly by using a mortar and pestle in a nitrogen glove box. Quantitative analysis of oxalate formation was performed by volumetric titrations by using standardized KMnO<sub>4</sub> solutions<sup>[22,23]</sup> as well as by ion chromatography methods for analysis of formate and oxalate.

## Acknowledgements

Georgian Court gratefully acknowledges funding from Liquid Light, Inc., for the undergraduate students who helped to conduct the experimental work for this paper. V.S.B. acknowledges the AFOSR grant FA9550-13-1-0020 and high performance computing facilities from NERSC and Yale University.

**Keywords:** carbon · carbon dioxide fixation · density functional calculations · reactive intermediates · reduction

- [1] M. Aresta, A. Dibenedetto, *Dalton Trans.* **2007**, 2975–2992.
- [2] E. J. Quadrelli, G. Centi, J. Duplan, S. Perathoner, *ChemSusChem* **2011**, *4*, 1194–1215.
- [3] A. Paparo, J. S. Silvia, E. C. Kefalidis, T. P. Spaniol, L. Maron, J. Okuda, C. C. Cummins, *Angew. Chem. Int. Ed.* **2015**, *54*, 9115–9119; *Angew. Chem.* **2015**, *127*, 9243–9247.
- [4] J. Andrez, J. Pacaut, P. Bayle, M. Mazzanti, *Angew. Chem. Int. Ed.* **2014**, *53*, 10448–10452; *Angew. Chem.* **2014**, *126*, 10616–10620.
- [5] X. Min, M. W. Kanan, *J. Am. Chem. Soc.* **2015**, *137*, 4701–4708.
- [6] J.-P. Jones, G. K. S. Prakash, G. A. Olah, *Isr. J. Chem.* **2014**, *54*, 1451–1466.
- [7] J. D. Watkins, A. B. Bocarsly, *ChemSusChem* **2014**, *7*, 284–290.
- [8] D. Kopljar, A. Inan, P. Vindayar, N. Wagner, E. Klemm, *J. Appl. Electrochem.* **2014**, *44*, 1107–1116.
- [9] R. Angamuthu, P. Byers, M. Lutz, A. L. Spek, L. Anthony, E. Bouwman, *Science* **2010**, *327*, 313–315.
- [10] N. Hollingsworth, R. S. F. Taylor, M. T. Galante, J. Jacquemin, C. Longo, K. B. Holt, N. H. de Leeuw, C. Hardacre, *Angew. Chem. Int. Ed.* **2015**, *54*, 14164–14168; *Angew. Chem.* **2015**, *127*, 14370–14374.
- [11] J. Kaczur, T. Kramer, K. Keyshar, P. Majsztrik, Z. Twardowski, "Process and High Surface Area Electrodes for the Electrochemical Reduction of Carbon Dioxide", Patent: US 8,858,777, 14 Oct 2014.
- [12] J. Kaczur, T. Kramer, K. Keyshar, P. Majsztrik, Z. Twardowski, "System and Process and High Surface Area Electrodes for the Electrochemical Reduction of Carbon Dioxide", Patent: US 2013/0105304, 2 May 2013.
- [13] J. Kaczur, K. Teamey, "Integrated Process for Producing Carboxylic Acids from Carbon Dioxide", Patent: US 9,085,827, 21 Jul 2015.
- [14] J. Kaczur, K. Teamey, "Integrated Process for Producing Carboxylic Acids from Carbon Dioxide", Patent: US 9,175,407, 3 Nov 2015.
- [15] M. C. Boswell, J. V. Dickson, *J. Am. Chem. Soc.* **1918**, *40*, 1779–1786.
- [16] E. H. Leslie, C. D. Carpenter, *Chem. Metall. Eng.* **1920**, *22*, 1195–1197.
- [17] R. Canning, M. A. Hughes, *Thermochim. Acta* **1973**, *6*, 399–409.
- [18] T. Meisel, Z. Halmos, K. Seybold, E. Pungor, *J. Therm. Anal.* **1975**, *7*, 73–80.
- [19] P. Baraldi, *Spectrochim. Acta Part A* **1979**, *35*, 1003–1007.
- [20] A. Górski, A. D. Kraśnicka, *J. Therm. Anal.* **1987**, *32*, 1895–1904.
- [21] A. Górski, A. D. Kraśnicka, *J. Therm. Anal.* **1987**, *32*, 1345–1354.
- [22] R. M. Fowler, H. A. Bright, *J. Res. Natl. Bur. Stand. (U. S.)* **1935**, *15*, 493–501.
- [23] D. C. Harris, *Quantitative Chemical Analysis*, 9th ed., W. H. Freeman and Company, New York, **2016**, pp. 146–148.

Received: June 24, 2016

Published online on October 26, 2016